GREENSTICK FRACTURES OR HOW PLANT BRANCHES, YOUNG MAMMAL BONES AND COMPOSITE PULTRUDED RODS BREAK

G. Vargas [a*], F. Mujika[a]

[a] *'Materials + Technologies' Group, Department of Mechanical Engineering, Polytechnic School, Universidad País Vasco/Euskal Herriko Unibertsitatea, Plaza Europa 1, 20018. Donostia-San Sebastián, Spain*
**gustavo.vargas@ehu.es*

Keywords: Biomechanics, Anisotropic materials, Greenstick fracture, Bending loading.

Abstract
Analytical models and experimental work for studying anisotropic beams subjected to flexural loading is presented. Particularly, the paper analyses the greenstick fracture mode on anisotropic curved beams, such as plant branches, young mammal bones and composite pultruded rods. Analytical approach considers all stress components. Circumferential normal stress is determined considering classical beam theory, and radial and out-of-plane shear stresses can be predicted by using the Airy's stress function. Experimental work has been carried out on unidirectional fibre reinforced plastic beams (pultruded rods with longitudinally oriented fibres). Three and four-point bending tests have been implemented, considering several span-to-diameter ratios. Experimental conditions that promote a greenstick fracture mode on specimens have been considered.

1. Introduction

Considering a curved beam subjected to flexural loading, the stress state is composed by in-plane circumferential normal stress, in-plane shear stress, radial normal stress, and out-of-plane shear stress. In beams composed of isotropic engineering materials transverse (i.e. radial) stresses are negligible compared with longitudinal (i.e. circumferential) ones, and they do not affect the mechanism of failure. Therefore, traditional analysis of isotropic beams do not take into account these radial stresses.

Nevertheless, out-of-plane radial stresses must be considered when beams composed of anisotropic materials are studied. Fibre reinforced composites, both natural and man-made, are stronger and stiffer longitudinally than transversely, and consequently radial stresses due to bending can produce catastrophic failure. Thus, such radial stresses could enlighten the greenstick fracture behaviour of some anisotropic beams such as green branches and twigs, bones of young mammals, and uniaxially reinforced composite beams. A greenstick fracture is a partial, angled fracture where the convex side ruptures (without the fracture line traversing the beam), and the concave side bends [1]. On Figure 1 a greenstick fracture of a green branch is presented.

Wooden branches and trunks have higher longitudinal than transverse strength due to the alignment of the tracheids (fibre cells) along the stem axis; in the tangential direction there are

no oriented tracheids and as a result tangential is the weakest direction [2]. Mammalian lamellar bones are also anisotropic because of the orientation of collagen fibrils reinforced by hydroxyapatite platelets [3]. In addition, young bones are more flexible and more anisotropic than adult ones, where longitudinal stiffness is approximately twice as transverse one. Figure 2 displays greenstick incomplete fractures of young radius and ulna [4]. Man-made composite beams composed of unidirectional fibre reinforced plastics are also highly anisotropic materials with longitudinal-to-transverse strength ratios up to 40:1.

Figure 1. The so-called greenstick fracture of a branch: a break on the convex side before splitting down the middle, with large longitudinal cracks along the centre line.

Figure 2. Frontal (a) and lateral (b) greenstick fractures of the radius and ulna of a 5-year-old child. Fully broken cortex (🡐) on one side, and intact bone on the other side (⇨). From Lee et al. [4] with permission.

On that sense, analytical approaches and experimental work for studying greenstick fracture mode of anisotropic beams subjected to flexural loading is presented in this contribution. Analytical approach considers all stress components: radial and out-of-plane shear stresses, that can be predicted by using the Airy's stress function, previously determining circumferential normal stress by classical beam theory. Mechanical testing has been carried out by both three-point bending and four-point bending tests.

2. Analytical approach

2.1. In-plane stresses

Circumferential normal stress σ_θ has been considered for both three-point bending (3-PB) and four-point bending (4-PB). In Figure 3 the loading configuration for 4-PB is presented as well as the shear force Q and the bending moment M diagrams, considering an applied load P, a circular-cross section specimen with radius ρ, a support span S_o, and a loading span S_i. Shear force Q and bending moment M are:

$$Q = \frac{P}{2} \qquad M = \frac{P}{4}\left(S_o - S_i\right) \tag{1}$$

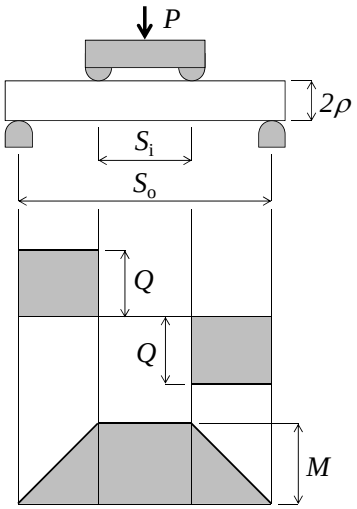

Figure 3. Four-point bending configuration, and the shear force *Q* and the bending moment *M* diagrams.

Three bending configurations have been analyzed: 3-PB set-up achieved for $S_i = 0$, 4-PB one-third span set-up completed for $S_i = S_o/3$, and 4-PB one-half span set-up attained for $S_i = S_o/2$. According to classical beam theory (CBT), the maximum circumferential stress $\sigma_{\theta max}$ is:

$$\sigma_{\theta\,\max} = k_1 \frac{PL}{\pi \rho^3} \tag{2}$$

where k_1 depends on bending set-up, as presented in Table 1.

Bending set-up	k_1	k_2	k_3	k_4	k_5	k_6
3-PB	1	1/48	5/18	1/48	1/12	10/3
4-PB-1/3	2/3	23/1296	5/27	5/324	5/81	3
4-PB-1/2	1/2	11/768	5/36	1/96	1/24	10/3

Table 1. Constants related to analytical approach for bending configurations: three-point bending (3-PB), four-point bending one-third span (4-PB-1/3), and four-point bending one-half span (4-PB-1/2).

2.2. Stiffness

Regarding the stiffness of circular-cross section beams, the deflection at the mid-span δ_{MS} and the deflection at loading points δ_{LP}, can be derived assuming that CBT applies [5] considering the effect of both bending moment and shear force, having a shear correction factor for circular-cross sections equal to 10/9 [6]:

$$\delta_{MS} = k_2 \frac{P S_o^{\,3}}{E_f I} + k_3 \frac{P S_o}{G A} \tag{3}$$

$$\delta_{LP} = k_4 \frac{P S_o^{\,3}}{E_f I} + k_3 \frac{P S_o}{G A} \tag{4}$$

where k_2, k_3, and k_4 depends on bending configuration, as displayed in Table 1, E_f is the flexure modulus on the fibre direction (axial), G is the in-plane shear modulus, I is the moment of inertia with respect to the middle plane, and A is the cross-sectional area.

According to Eq. (4) it is possible to obtain experimentally the flexure modulus E_f and the in-plane shear modulus G, considering two different support spans (solving a 2 x 2 system of equations) based on the applied load vs. loading point deflection curve. For circular-cross section beams, the slope δ_{LP}/P can be derived from Eq. (4) as follows:

$$\frac{\delta_{LP}}{P} = \frac{k_5}{\pi}\frac{{S_o}^3}{\rho^4}\left[\left(\frac{1}{E_f}\right) + k_6\left(\frac{\rho}{S_o}\right)^2\left(\frac{1}{G}\right)\right] \tag{5}$$

where k_5 and k_6 vary for each flexure configuration, as given in Table 1.

2.3. Out-of-plane stresses

Airy's stress function ϕ in polar coordinates [7] relates three components of stress: in-plane circumferential stress σ_θ, out-of-plane radial stress σ_r, and out-of-plane shear stress $\tau_{r\theta}$. The stress components obtained from this stress function satisfy equilibrium conditions in the considered domain, and they can be expressed as follows:

$$\sigma_r = \frac{1}{r}\frac{\partial\phi}{\partial r} + \frac{1}{r^2}\frac{\partial^2\phi}{\partial\theta^2} \tag{6a}$$

$$\sigma_\theta = \frac{\partial^2\phi}{\partial r^2} \tag{6b}$$

$$\tau_{r\theta} = \frac{1}{r^2}\frac{\partial\phi}{\partial\theta} - \frac{1}{r}\frac{\partial^2\phi}{\partial r\,\partial\theta} \tag{6c}$$

After determining the in-plane circumferential stresses σ_θ, it is possible to determine the Airy's stress function in polar coordinates from Eq. (6b), accomplishing several integrations. Equations are expressed as function of the radial coordinate r and circumferential coordinate θ, as shown in Figure 4. Then the two out-of-plane stresses, σ_r and $\tau_{r\theta}$, can also be determined from the other Airy's stress function equations, that is Eq. (6a) and Eq. (6c), respectively.

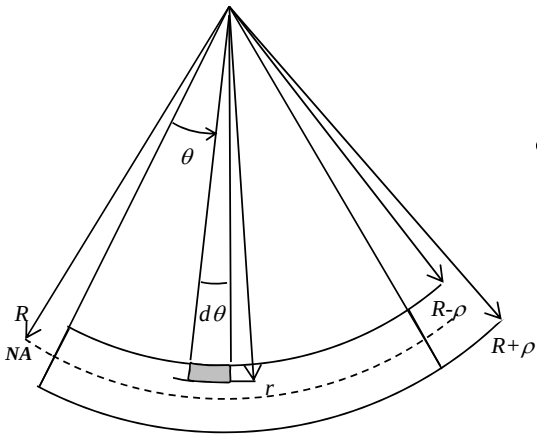

Figure 4. Radial and circumferential variables of the beam.

3. Experimental work

3.1. Material and apparatus

Unidirectional fibre reinforced plastic beams (pultruded rods) were considered for experimental work due to the highly anisotropic mechanical behaviour. Composite circular cross-section rods consisted of vinylester resin reinforced with longitudinally oriented E-glass fibre, and were fabricated and kindly provided by Abeki Composites, S.L. Pultruded rods had a nominal diameter of 8 mm. A universal testing machine MTS - Insight 10 with a 10 kN load cell and standard bending test fixtures was used.

3.2. Fibre volume fraction

The fibre volume fraction of the laminates has been determined through the ignition loss method (or burn-out technique) according to ASTM D 2584 - 11 [8]. The determination of fibre volume fraction requires the measurement of the composite density, which was measured in accordance with ASTM D 792 - 08 [9], considering that the void content is negligible. Experimental results reveal that fibre volume fraction and density of composite rods were 58.6 % and 2.02 g/cm^3, respectively.

3.3. Bending test

Three-point bending (3-PB), four-point bending one-third span (4-PB-1/3), and four-point bending one-half span (4-PB-1/2) tests have been performed considering different support span-to-diameter ratios. The nominal support span S_o, the nominal loading span S_i, and support span-to-diameter ratios $S_o/(2\rho)$ considered are consigned in Table 2, as depicted in Figure 3.

For determining the flexure modulus E_f, five specimens were loaded considering as strain limits 0.1% and 0.3%. In the case of circumferential strength X_θ specimens were loaded until first-ply failure defined as the first deviation in the load-deflection curve. A minimum overhang of 10 % of the support span at each extreme fixture, in accordance with ASTM D 4476 - 09 [10], must be taken into account. The load was applied at a stress rate of 250 - 350 MPa/min in the outer fibres of the specimen as recommended by ACI 440 for tensile tests of FRP rods [11]. The loading point displacement rates δ'_{LP} are consigned in Table 2.

Bending set-up	S_o **(mm)**	S_i **(mm)**	$S_o/(2\rho)$	δ'_{LP} **(mm/min)**
3-PB	64	0	8	0.533 – 0.747
	96	0	12	1.200 – 1.680
	128	0	16	2.133 – 2.987
	200	0	25	5.208 – 7.292
4-PB-1/3	72	24	9	0.750 – 1.050
	96	32	12	1.333 – 1.867
	128	42,67	16	2.370 – 3.319
	200	66,67	25	5.787 – 8.102
4-PB-1/2	64	32	8	0.533 – 0.747
	96	48	12	1.200 – 1.680
	128	64	16	2.133 – 2.987
	200	100	25	5.208 – 7.292

Table 2. Testing parameters for bending tests: three-point bending (3-PB), four-point bending one-third span (4-PB-1/3), and four-point bending one-half span (4-PB-1/2).

4. Discussion and results

4.1. Flexure modulus and shear modulus

Flexure modulus E_f experimental results, consigned in Table 3, reveal that there is no appreciable difference between the considered bending methods (i.e. 3PB, 4PB-1/3, 4PB-1/2). Hence, it can be concluded that the analysis carried out by CBT can be considered suitable.

However, shear modulus G experimental results (Table 3) exhibit a considerable difference (nearly 20 %) between the three bending methods. This fact is due to shear effects. Contrasting shear force diagrams (Figure 3), it can be inferred that as loading span increases shear effects decrease. It can also be noticed comparing shear deflection with bending deflection, the two terms on Eqs. (3) and (4). On that sense, shear effects are higher on three-point bending and they are lower in four-point bending one-half span.

4.2. Circumferential strength

As in the case of flexure modulus results, circumferential strength X_θ results given at first rupture of outer fibres, displayed in Table 3, expose no significant differences between the considered bending methods. The testing conditions correspond to a support span of 128 mm, $S_o/(2\rho) = 16$. Besides strength results, the ultimate fibre strain of outer fibres at failure load, $\varepsilon_{\theta u}$, and displacement at loading points at first breaking of outer fibres δ_{LPu}, are consigned.

Bending set-up	E_f **(MPa)**	G **(MPa)**	X_θ **(MPa)**	$\varepsilon_{\theta u}$ **(%)**	δ_{LPu} **(mm)**
3-PB	50292 ± 479	1221 ± 64	822	2.06	7.42
4-PB-1/3	50898 ± 361	1148 ± 45	917	2.29	8.49
4-PB-1/2	51070 ± 110	1005 ± 14	837	2.09	6.98

Table 3. Experimental results of flexure modulus E_f, shear modulus G, and circumferential strength X_θ.

4.3. Failure mode

Figures 5 and 6 show the two flexure failure modes presented in FRP rods after bending tests. Figure 5 displays a 3PB brittle failure observed in all 3PB tests for all support spans, having maximum displacement at loading points-to-span ratios up to 8.86 %. In the case of 4PB with one- half span the failure mode was brittle in the case of low support span (i.e. S_o = 128 mm), and ductile for the high support span (i.e. S_o = 200 mm), as presented in Figure 6. The ductile mode was characterized by ratios between maximum displacement at loading points and support span up to 8.79 %.

The brittle failure of the specimen starts with rupture of fibres on the convex side of the loading section; subsequently such rupture extended into a vertical crack toward the concave side. On ductile failure mode the tensile stress on the convex side develops the rupture of fibres; afterwards broken fibres delaminate when shear stresses exceeded the bond strength between fibres polymeric matrix, as reported by Zhang et al. [12]. The ductile failure mode is known as greenstick fracture: limited fibre ruptures on the convex tensile side followed by large longitudinal cracks along the centre line [1].

Regarding the deflection of the composite beams, expressed on Eqs. (3) and (4), there are two components: one due to bending moment and other one due to shear force. Shear deflection

compared to bending deflection can be considered negligible for a support span-to-diameter ratio equal to 25 and a flexure modulus-to-shear modulus ratio higher than 40. After that, the beam deflection is mainly due to bending load. Starting from the deflection at loading points for 4PB cases, the deflection at the mid-span can be estimated based on CBT. Afterwards, for a maximum displacement at loading points-to-support span ratio equal to 8.79 % the maximum displacement at mid-span-to-support span ratio reaches to 12.08 %. Consequently, only the 4PB-1/2 tests with $S_o/(2\rho)$ = 25 have been carried out under great displacements condition, having in mind that the small displacements condition requires a δ_{max}/S_o ratio less than 10 % [13]. Precisely, in a bending situation under great displacements the out-of-plane stresses could have a significant influence, requiring a further analysis based on the Airy's stress function, as described in Section 2.3.

Figure 5. Failure mode of pultruded rods under 3-PB (support span-to-diameter ratio = 25).

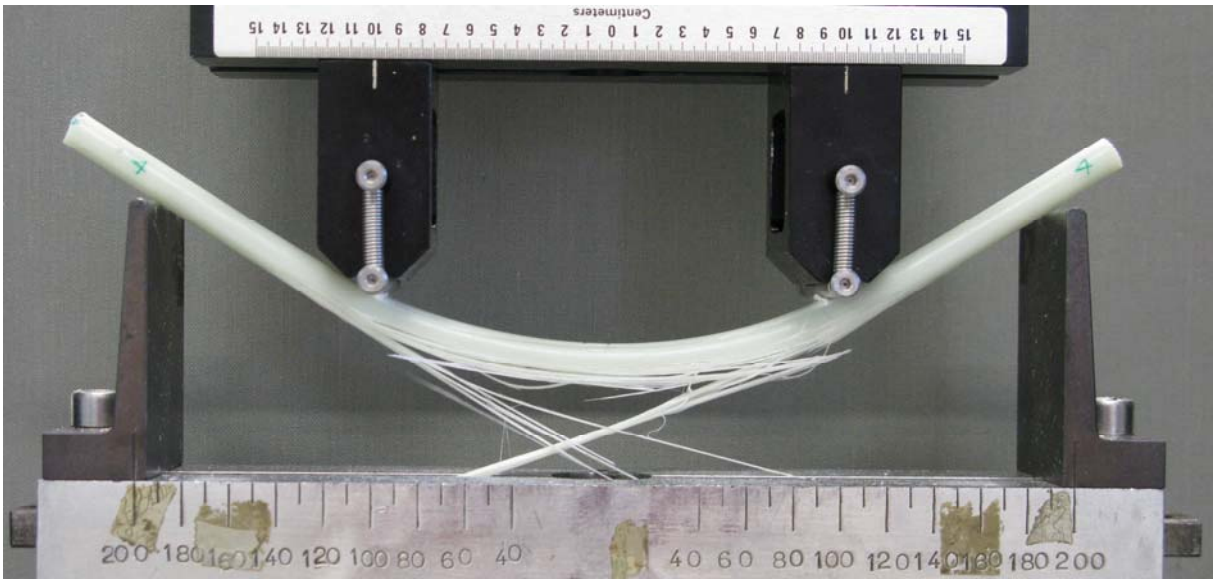

Figure 6. Failure mode of pultruded rods under 4-PB one-half span (support span-to-diameter ratio = 25).

5. Conclusions

In the present contribution analytical approaches an experimental work for studying initially straight beams of unidirectional fibre reinforced plastic subjected to flexural loading have been presented. The aim of the paper was to evaluate the greenstick fracture mode presented in some anisotropic beams such as plant branches, young mammal bones and composite pultruded rods with longitudinally oriented fibres. The analytical approach has been divided in two parts: first of all circumferential normal stress has been calculated from classical beam theory; subsequently it is possible to determine both the Airy's stress function, and after that the unknown out-of-plane stress components that satisfy equilibrium conditions in the considered domain: radial normal and out-of-plane shear stresses.

Experimental work has been performed under three-point and four-point bending conditions, and several support span-to-diameter ratios have been considered. Brittle failures, characterized by a rupture of fibres that starts on the bottom side of the loading section and quickly develops into a vertical crack toward the upper side, have been presented in all tested specimens under 3PB loading. 4PB one- half span specimens presented two failure modes: brittle mode for a small support span, $S_o/(2\rho) = 16$, and ductile one for a high support span, $S_o/(2\rho) = 25$. Such ductile failure was carried out under great displacements condition, which is known as greenstick fracture, where limited fibre ruptures on the convex tensile side are followed by large longitudinal cracks along the centre line.

References

[1] A. R. Ennos and A. van Casteren. Transverse stresses and modes of failure in tree branches and other beams. *Proceedings B of the Royal Society*, 277:1253-1258, 2010.

[2] A. Reiterer, I. Burgert, G. Sinn and S. Tschegg. The radial reinforcement of the wood structure and its implication on mechanical and fracture mechanical properties - A comparison between two tree species. *Journal of Materials Science*, 37(5):935-940, 2002.

[3] J. W. C. Dunlop and P. Fratzl. Biological Composites. *Annual Review of Materials Research*, 40:1-24, 2010.

[4] P. Lee, T. B. Hunter and M. Taljanovic. Musculoskeletal colloquialisms: how did we come up with these names? *RadioGraphics*, 24(4):1009-1027, 2004.

[5] S. Timoshenko. *Strength of materials. Part I*. Van Nostrand, Lancaster, 1948.

[6] W. D. Pilkey. *Formulas for stress, strain, and structural matrices*. 2nd ed. Wiley, Hoboken, 2005.

[7] S. P. Timoshenko and J. N. Goodier. *Theory of elasticity*. McGraw-Hill, New York, 1951.

[8] ASTM ASTM D 2584 - 11. Standard Test Method for Ignition Loss of Cured Reinforced Resins. *Annual Book of ASTM Standards*. 83.080.10, 2011.

[9] ASTM D 792 - 08. Standard Test Methods for Density and Specific Gravity (Relative Density) of Plastics by Displacement. *Annual Book of ASTM Standards*. 83.080.01, 2008.

[10] ASTM D 4476 – 09. Standard Test Method for Flexural Properties of Fiber-Reinforced Pultruded Plastic Rods. *Annual Book of ASTM Standards*. 08.02, 2009.

[11] ACI 440K. Guide Test Methods for Fiber-Reinforced Plastic (FRP) Rods and Sheets. *American Concrete Institute*. ACI Committee 440, 2004.

[12] B. Zhang, R. Masmoudi, and B. Benmokrane. New method for testing fiber-reinforced polymer rods under flexure. *Journal of Testing and Evaluation*, 35(2):1-6, 2006.

[13] ISO 14125:1998. Fibre-reinforced Plastic Composites, Determination of Flexural Properties. *International Organization for Standardization*, 1998.